

Phenomenological approach to 3D spinning waves

D.V. STRUNIN AND S.A. SUSLOV

*Department of Mathematics and Computing, University of Southern Queensland,
Toowoomba, Queensland 4350, Australia*
e-mail: strunin@usq.edu.au, ssuslov@usq.edu.au

Abstract

The spinning waves occur in solid flames and detonation when the plane uniformly propagating reaction front loses stability. As a result, the front breaks into localized zones of intensive reaction. We study a 3D phenomenological model aimed at modeling such phenomena. The model constitutes a nonlinear partial differential equation. This work contains preliminary results demonstrating the capacity of the model to reproduce basic experimental features of the unstable front: metastability of the uniform state and formation of self-sustained regime with predominantly lateral propagation of the front curvature.

1 Introduction

Spinning combustion is an interesting nonlinear phenomenon initially discovered in detonation [1] and later on in solid-phase combustion [2]. One should distinguish the meaning of the term “nonlinearity” when applied to combustion from its meaning when applied to waves in fluids and other conservative systems. Roughly speaking, small amplitude waves in fluids are linear and the nonlinear effects become significant when the amplitude is relatively large. Any combustion wave is already nonlinear by its nature. However, small perturbations to the traveling wave solution of the original reaction-diffusion equations satisfy linearized equations. If instability develops, the nonlinear effects come into play.

The spinning waves in solid-phase combustion were extensively studied since the early 1970’s experimentally [2, 3, 4] and theoretically [5, 6, 7, 8] and still attract considerable attention [9, 10].

In the present paper we model the nonlinear effects with the phenomenological partial differential equation. Previously, a one-dimensional (involving one independent spatial variable) version of the equation was formulated [11]:

$$\partial_t H = \partial_x^6 H - \partial_x^2 H (\partial_x H)^2 + (\partial_x H)^4, \quad (1)$$

where H is the coordinate of the combustion front which is assumed to be a line separating fresh mixture above it from hot products below. In other words, $H(x, t)$ is the distance traveled by the front through the reacting mixture, depending on the time t and coordinate x transversal to the average propagation.

In deriving model (1) the goal was to reproduce three main qualitative features of the actual process. First, the decay of a front with relatively smooth curvatures. This would correspond to the decay of a front with insufficient initial concentration of energy. Second, the self-sustained non-trivial dynamics of a front with relatively sharp curvatures so that a typical amplitude of the settled curvatures is governed by the equation, not the initial condition. Third, the self-propagating front moving predominantly in lateral direction at any particular moment. These properties are ensured by the dynamical structure of (1): the purely dissipative linear part, nonlinear nature of the source and overall dynamical balance involving all three terms in the right-hand side. equation (1) was shown to give spinning wave solutions corresponding to the front moving around a hollow cylinder with thin walls [11].

2 Three-dimensional model

Here we generalize equation (1) to incorporate the second transversal dimension, y , in order to model the front propagation through a 3D continuum. With the distance H measured along the third axis, z , we aim to obtain a three-dimensional pattern. The generalization is:

$$\partial_t H = \nabla^6 H - \nabla^2 H (\nabla H)^2 + (\nabla H)^4, \quad (2)$$

where

$$\nabla = \mathbf{i} \partial_x + \mathbf{j} \partial_y.$$

For simplicity we use a square domain, $0 < x, y < L$, corresponding to a rod with a constant square cross section. When running numerical

experiments we found it convenient to use a modified form of equation (2) with some arbitrary positive coefficients included in each term in the right-hand side:

$$\partial_t H = a \nabla^6 H - b \nabla^2 H (\nabla H)^2 + c (\nabla H)^4. \quad (3)$$

Equation (2) is transformed into (3) by rescaling H , t and the spatial coordinates. In Cartesian coordinates (3) has the form

$$\begin{aligned} \partial_t H = & a \left(\partial_x^6 H + 3 \partial_x^4 \partial_y^2 H + 3 \partial_x^2 \partial_y^4 H + \partial_y^6 H \right) && \text{dissipation} \\ & - b \left(\partial_x^2 H + \partial_y^2 H \right) \left[(\partial_x H)^2 + (\partial_y H)^2 \right] && \text{source} \\ & + c \left[(\partial_x H)^4 + 2 (\partial_x H)^2 (\partial_y H)^2 + (\partial_y H)^4 \right]. && \text{transfer} \end{aligned} \quad (4)$$

On the right, we label the terms according to their dynamical action (for more detail see [11]). The following conditions are adopted:

$$\begin{aligned} \partial_x H = 0, \quad \partial_x^2 H = 0, \quad \partial_x^3 H = 0 & \quad \text{at } x = 0 \text{ and } x = L, \\ \partial_y H = 0, \quad \partial_y^2 H = 0, \quad \partial_y^3 H = 0 & \quad \text{at } y = 0 \text{ and } y = L. \end{aligned} \quad (5)$$

The zero first derivatives stipulate zero slope of the front towards the boundaries and therefore these conditions are associated with the physical condition of adiabaticity. The other conditions are imposed arbitrarily at this stage.

3 Numerical results

Equation (4) was discretised in space on a uniform equilateral grid using standard second order accurate central differences using 7×7 point stencil which allows to preserve the symmetry of the original equation in approximating all required derivatives including the mixed ones. The boundary conditions (5) were discretised using the fictitious point approach. The essence of this technique is in introducing a number (3 in this case) of additional layers of discretization points just outside of each of the boundaries. Then formally the physical boundary points are treated as interior and therefore equation (4) is approximated uniformly up to and including the physical boundaries. Boundary conditions (5) are then approximated using second order central

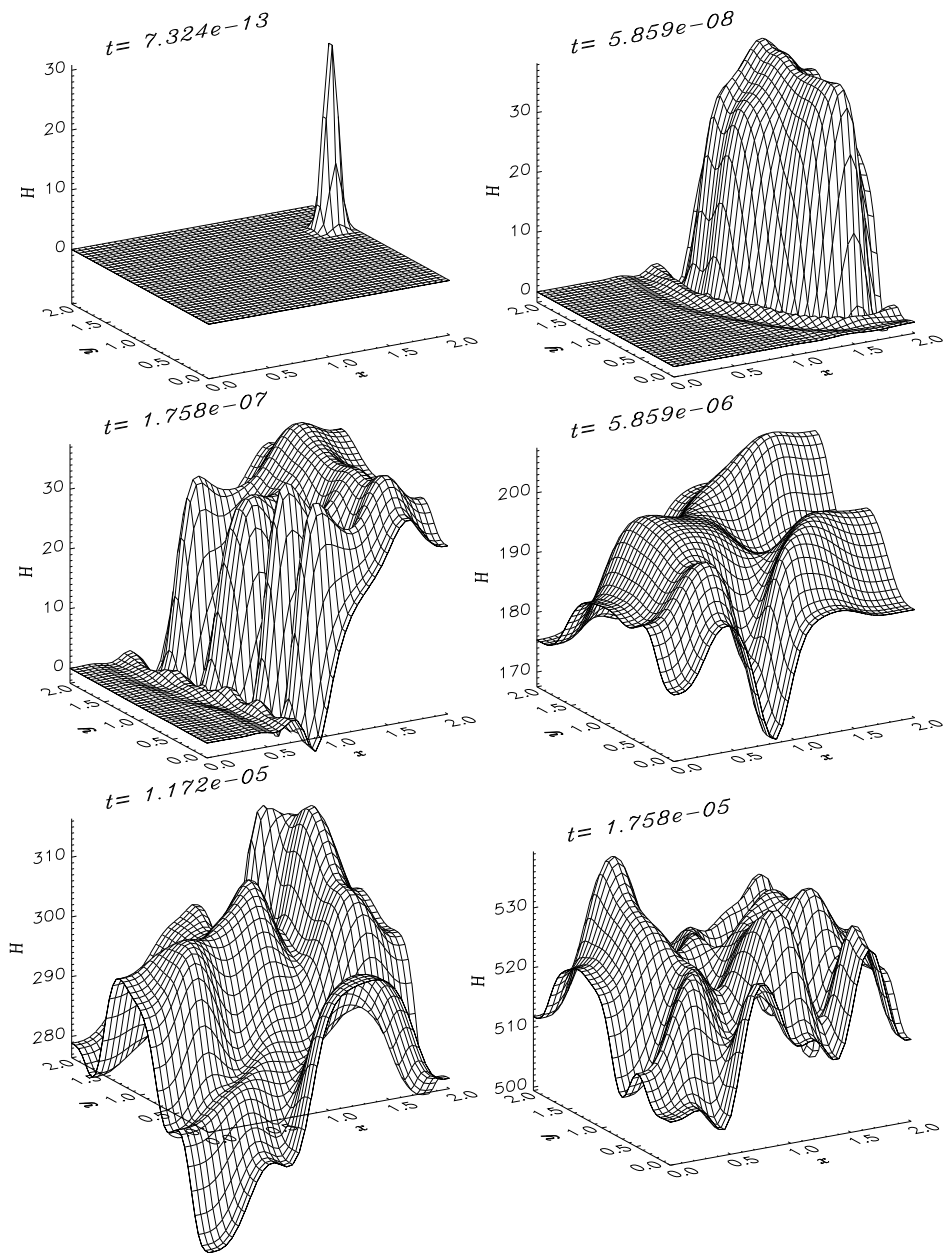


Figure 1: Numerical solution of equation (4) with boundary conditions (5) and initial pulse of magnitude $H_0 = 35$ near the top right corner of the domain for $a = c = 1$ and $b = 10$.

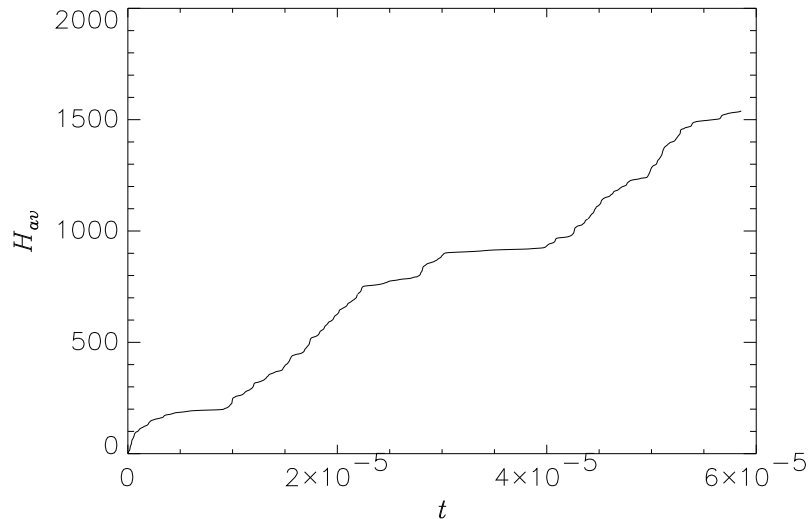


Figure 2: Average front position as a function of time. Parameters as in Figure 1.

finite differences and the resulting equations are used to eliminate the fictitious points in favor of the interior points adjacent to the boundary. This approach enables one to preserve the symmetry and the second order spatial accuracy up to and including the boundaries. This would not be possible to do using one-sided differences near the boundaries. Since equation (4) is nonlinear, to avoid expensive iterative solution of a system of nonlinear difference equations at each time step an explicit first order accurate forward Euler method was chosen for time discretization. To avoid numerical instability in time integration a sufficiently small time step was used. It was found that for the spatial discretization steps of $\Delta x = \Delta y = 0.025$ (for which the numerical solution was obtained) the time step $\Delta t = 0.003\Delta x^6$ was sufficiently small to ensure numerical stability for all regimes including a very stiff initial stage with an initial condition of the form of a δ -function placed asymmetrically near the top right corner $(x, y) = (2, 2)$ of the domain, see the first plot in Figure 1. For the chosen set of parameters and geometry, despite the high symmetry of both the original equation and the adopted discretization scheme, the solution obtained from a slightly asymmetric initial state never becomes symmetric. Due to the nonlinearity the

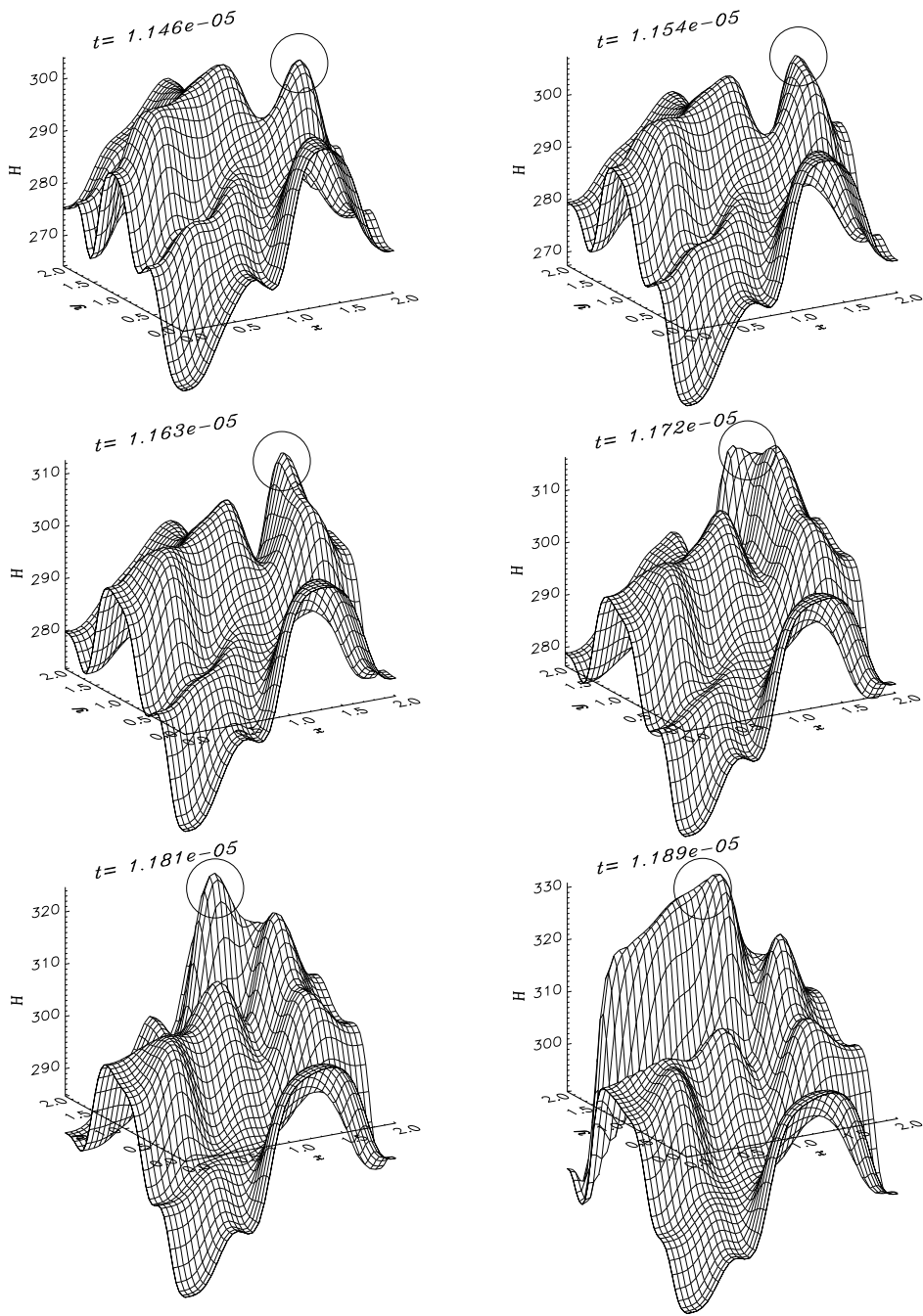


Figure 3: Counterclockwise spinning wave (circled) in the numerical solution of equation (4). Parameters as in Figure 1.

relatively smooth initial front seen in the second snapshot in Figure 1 becomes unstable and develops secondary fronts as seen in the third snapshot. The nonlinear interaction of these multiple secondary fronts in turn leads to what appears to be chaotic dynamics for sufficiently large time, see snapshots 4–5 in Figure 1. Despite this overall chaotic behavior of a solution the average position of a front H_{av} always increases with time as shown in Figure 2 which confirms the relevance of the proposed model to realistic situation of a propagating combustion front. The dynamics of H_{av} shows that the front propagates with a non-constant speed with periods of slow laminar burning dominated by the diffusion terms in equation (4) followed by a rapid turbulent combustion largely determined by interactions of curvilinear fronts described by nonlinear terms in equation (4). The computations were performed up to time $t \approx 5.9 \times 10^{-5}$ (80 millions time steps) and show that the front evolution for the chosen set of parameters remains intermittently chaotic. However a closer look at some intermediate stages of the front evolution indicates that model (4) admits shortlived solutions representing spinning waves which propagate along the boundaries of the domain. A series of snapshots presented in Figure 3 show a front (circled) propagating along the boundaries counterclockwise for some time before this motion is destroyed by nonlinear collisions with other local fronts corresponding to the maxima of the presented solution.

4 Conclusions

We presented selected results on 3D modeling of unstable combustion waves using the phenomenological model (4). Using numerical simulations we showed that the model preserves the property of metastability of an initially uniform front. When excited by a sufficiently strong perturbation the front forms a self-sustained structure moving predominantly in lateral direction. Such a motion is typical for spinning waves signs of which were detected in the presented numerical solution. However the obtained spinning waves are easily destroyed by collisions with other nonlinear local fronts. It is hoped that stable spinning solutions can be obtained from the suggested model by choosing carefully the appropriate set of model parameters and initial conditions.

References

- [1] Zel'dovich, Ya.B. and Kompaneets, A.S., *Theory of Detonation*. New York: Academic Press, 1960.
- [2] Merzhanov, A.G., Filonenko, A.K. and Borovinskaya, I.P., New phenomena in combustion of condensed systems. *Doklady Phys. Chem.*, 1973, vol. 208, pp. 122–125.
- [3] Dvoryankin, A., Strunina, A.G. and Merzhanov, A.G., Trends in the spin combustion of thermites. *Combust. Explos. Shock Waves*, 1982, vol. 18, pp. 134–139.
- [4] Strunin, D.V., Strunina, A.G., Rumanov, E.N. and Merzhanov, A.G., Chaotic reaction waves with fast diffusion of activator, *Phys. Lett. A*, 1994, vol. 192, pp. 361–363.
- [5] Ivleva, T.P., Merzhanov, A.G. and Shkadinsky, K.G., Principles of the spin mode of combustion front propagation. *Combust. Explos. Shock Waves*, 1980, vol. 16, pp. 133–139.
- [6] Aldushin, A.P., Malomed, B.A. and Zel'dovich, Ya.B., Phenomenological theory of spin combustion. *Combust. Flame*, 1981, vol. 42, pp. 1–6.
- [7] Volpert, V.A., Volpert, A.I. and Merzhanov, A.G., Application of the theory of bifurcations in study of the spinning combustion waves. *Doklady Akad. Nauk SSSR*, 1982, vol. 262, pp. 642–645.
- [8] Novozhilov, B.V., On the theory of the surface spin combustion. *Doklady Ross. Akad. Nauk*, 1992, vol. 326, pp. 485–488.
- [9] Ivleva, T.P., Private communication, 2002.
- [10] Ivleva, T.P. and Merzhanov, A.G., Mathematical simulation of three-dimensional unstable solid-flame combustion, *Proc. of Int. Conf. on Combustion and Detonation. Zel'dovich Memorial II*, Moscow, 2004.
- [11] Strunin, D.V., Autosoliton model of the spinning fronts of reaction. *IMA J. Appl. Math.*, 1999, vol. 63, pp. 163–177.